Cholesterol Depletion Suppresses the Translational Diffusion of Class II Major Histocompatibility Complex Proteins in the Plasma Membrane

Marija Vrljic,* Stefanie Y. Nishimura,† W. E. Moerner,*† and Harden M. McConnell*†
*Biophysics Program and †Department of Chemistry, Stanford University, Stanford, California

ABSTRACT Glycosylphosphatidylinositol (GPI)-linked and native major histocompatibility complex class II I-E^k were used as probes to determine the effect of varying cholesterol concentration on the mobility of proteins in the plasma membrane. These proteins were imaged in Chinese hamster ovary cells using single-molecule fluorescence microscopy. Observed diffusion coefficients of both native and GPI-linked I-E^k proteins were found to depend on cholesterol concentration. As the cholesterol concentration decreases the diffusion coefficients decrease by up to a factor of 7 for native and 5 for GPI-linked I-E^k. At low cholesterol concentrations, after sphingomyelinase treatment, the diffusion coefficients are reduced by up to a factor of 60 for native and 190 for GPI-linked I-E^k. The effect is reversible on cholesterol reintroduction. Diffusion at all studied cholesterol concentrations, for both proteins, appears to be predominantly Brownian for time lags up to 2.5 s when imaged at 10 Hz. A decrease in diffusion coefficients is observed for other membrane proteins and lipid probes, $DiIC_{12}$ and $DiIC_{18}$. Fluorescence recovery after photobleaching measurements shows that the fraction of immobile lipid probe increases from 8 to ~40% after cholesterol extraction. These results are consistent with the previous work on cholesterol-phospholipid interactions. That is, cholesterol extraction destroys liquid cholesterol-phospholipid complexes, leaving solid-like high melting phospholipid domains that inhibit the lateral diffusion of membrane components.

INTRODUCTION

Mixtures of cholesterol and certain phospholipids have long been known to exhibit nonideal behavior. Changes in cholesterol concentration have been reported to have an effect on liquid-liquid phase separation in model lipid membranes, on the formation of complexes between cholesterol and phospholipids, as well as on the motion of membrane proteins in the plasma membrane (McConnell and Vrljic, 2003).

Although the plasma membrane is a complicated mixture of lipids and proteins, a large body of biochemical and microscopic evidence suggests that interactions of cholesterol with other lipids, as well as proteins, may govern organization of the plasma membrane into lipid domains. This has been extensively reviewed (Anderson, 1998; Anderson and Jacobson, 2002; Brown and London, 1998, 2000; Simons and Toomre, 2000; Subczynski and Kusumi, 2003).

Lipid domains are reported to be enriched in saturated lipids, sphingomyelin, cholesterol (Brown and Rose, 1992), glycosylphosphatidylinositol (GPI)-linked (Brown and Rose, 1992; Harder et al., 1998), palmitoyl-linked proteins, myristoyl-linked proteins (Arni et al., 1998; Moffett et al., 2000), and some transmembrane proteins (Harder and Kuhn, 2000; Scheiffele et al., 1997). Cholesterol appears to play a key role in organizing lipids into lipid domains. Reduction of the cholesterol concentration in the plasma membrane leads to the disappearance of detergent-resistant membrane (DRM) fractions, loss of signaling function, and resistance to cross-linking (Harder et al., 1998; Xavier et al., 1998; Field et al., 1997; Sheets et al., 1999; Vidalain et al., 2000). The spatial distribution and diffusion coefficients of some lipid analogs and proteins are different at normal and reduced cholesterol concentrations (Hao et al., 2001; Pralle et al., 2000; Dietrich et al., 2002; Kwik et al., 2003; Kenworthy et al., 2004; Shvartsman et al., 2003). The work of Pralle et al. (2000) and Shvartsman et al. (2003) suggested that at normal cholesterol levels, proteins found in the DRM fraction have lower diffusion coefficients than proteins found in the non-DRM fraction. At the reduced cholesterol level, the diffusion coefficients for all examined proteins were similar and corresponded to those of the non-DRM proteins. This result supports the model of lipid domains as distinct compartments within the membrane. In line with that model Dietrich et al. (2002) observed a reduction in the number of transient confinement zones after cholesterol depletion. In contrast, Hao and co-workers (2001) observed a uniform fluorescence intensity of $DiIC_{16}$, $DiIC_{12}$, and C_6-NBD-SM at normal cholesterol concentration and a nonuniform intensity at decreased cholesterol concentration. Based on fluorescence recovery after photobleaching (FRAP) measurements in areas enriched in the C_6-NBD-SM probe they found the diffusion of this lipid probe to be slower after cholesterol reduction. Kwik et al. (2003) reported an actin cytoskeleton-mediated increase in the immobile fraction of HLA I proteins upon reduction in cholesterol concentration, and Kenworthy et al. (2004) reported a decrease in the diffusion coefficients of both raft and nonraft proteins upon reduction in cholesterol. Yet other data seem to indicate that lowering the cholesterol concentration in the plasma membrane does not have an influence on the diffusion of fluorescent lipid

Submitted May 13, 2004, and accepted for publication October 19, 2004.

Marija Vrljic and Stefanie Y. Nishimura contributed equally to this work. Address reprint requests to Marija Vrljic, Dept. of Chemistry, Stanford University, Stanford, CA 94305-5080. Tel.: 650-723-4576; E-mail: marija@stanford.edu.

0006-3495/05/01/334/14 $2.00

doi: 10.1529/biophysj.104.045989

probe analogs (Fujiwara et al., 2002) or clustering of GPI-linked proteins and GM1 in microdomains (Kenworthy et al., 2000). A better understanding of such systems is needed before these contradictory data can be reconciled with one model of lipid domains.

In this work we have imaged the translational trajectories of native and GPI-linked I-E^k proteins in Chinese hamster ovary (CHO) cells, extending and substantiating an earlier report (Vrljic et al., 2003). Native I-E^k is a single-pass integral membrane protein. GPI-linked I-E^k has the same extracytoplasmic domain as native I-E^k, but the transmembrane and cytoplasmic domains have been replaced by the human placental alkaline phosphatase (PLAP) GPI anchor (Wettstein et al., 1991). Though structural analysis of human PLAP's GPI anchor in CHO cells has not been done, analysis of the PLAP phosphatidylinositol (PI) species from human term placentas suggested that PI species are 16:0-18:0 and 18:0-18:1 (Redman et al., 1994). In addition, the major GPI-derived PI species (including the ones from PLAP) in MDCK and FRT cells are 18:0-18:0 and minor PI species are 18:0-18:1 and 16:0-18:0. The latter was found primarily in FRT cells (Benting et al., 1999). PLAP expressed in MDCK and FRT cells localizes in the DRM fraction (Benting et al., 1999). I-E^k and other class II MHC alleles have been reported to exhibit hallmark properties of association with lipid domains. They reside in the DRM fractions (Huby et al., 1999; Anderson et al., 2000; Vrljic et al., 2002) and colocalize with other lipid raft markers after cross-linking (Hiltbold et al., 2003; Anderson et al., 2000; Huby et al., 1999), and signaling by class II molecules (Huby et al., 1999), as well as antigen presentation to T cells (Anderson et al., 2000), is disrupted by reduction of the cholesterol concentration.

The trajectories were imaged using a single-molecule epifluorescence imaging technique (Moerner and Fromm, 2003). Diffusion trajectories of native and GPI-linked I-E^k proteins at a normal plasma membrane cholesterol concentration have been extensively analyzed, and their motion was shown to be predominantly Brownian (Vrljic et al., 2002). Here we investigate the effect of modulating the plasma membrane cholesterol concentration on the motion of these proteins.

It is worth emphasizing here that our experiments were carried out at 22°C rather than 37°C. In retrospect this has turned out to be a fortunate choice from an experimental point of view since the large effects of cholesterol depletion on diffusion are likely to be magnified at the lower temperature.

MATERIALS AND METHODS

Cell culture

For details of cell culture, see our previous work (Vrljic et al., 2002). CHO cells transfected with either mouse MHC class II protein I-E^k (CHO-I-E^k) or with I-E^k extracytoplasmic domain fused with GPI-linker (CHO-GPI linked I-E^k) were a generous gift of M. M. Davis (Wettstein et al., 1991). During the course of this work cells were cultured in different lots of fetal calf serum (FCS) from different providers. Two lots were from HyClone (Logan, UT) and two from Gibco BRL (Carlsbad, CA). Different FCS did not affect the overall trend of the data, but did influence the values of the diffusion coefficients (Fig. S1 *D* in Supplementary Material). Two lots from HyClone resulted in values very close to one another, whereas two lots from Gibco gave rise to results that differed from one another and from HyClone sera.

Imaging conditions (cells)

For details, see our previous work (Vrljic et al., 2002). Briefly, cells were cultured on a chambered coverglass (Nalge Nunc International, Naperville, IL) and imaged in supplemented RPMI 1640 phenol red-free medium with an enzymatic oxygen scavenger system: 1% v/v glucose (Sigma, St.Louis, MO; 500 mg/ml stock), 1% v/v glucose oxidase (Sigma; 5000 U/ml stock), 1% v/v catalase (Sigma; 40,000 U/ml stock) and 0.5% v/v 2-mercaptoethanol (Sigma; 14.3 M stock). After addition of oxygen scavengers the chambered coverglass was sealed with parafilm ''M''. CHO cells can cycle between aerobic and anaerobic metabolism without effects on their viability for at least up to 60 min (data not shown; Rabinowitz et al., 1998a). Supplemented RPMI either did or did not contain 10% FCS. Absence of serum during imaging lowers the background, but does not affect the values of diffusion coefficients (data not shown). Data in the figures is an average of the data obtained in the presence and absence of FCS. Imaging was done at 22°C for up to 1 h, whereas treatments with different drugs before imaging were done at 37°C. Cells were labeled by incubation with 0.05–0.5 μg/ml Cy5-MCC 95-103 peptide for 15–30 min at 37°C.

Estimation of the cholesterol and sphingomyelin concentration

Total cell cholesterol was estimated using the cholesterol oxidase-based Amplex Red Cholesterol Assay Kit (Molecular Probes, Eugene, OR). Cholesterol esterase was omitted from the assay to exclude intracellular cholesterol esters. For all assays, the number of moles per cell of β-cyclodextrin (β-CD) or cholesterol-loaded methyl-β-cyclodextrin (chol-mβ-CD) matched the values used in microscopy experiments. All cholesterol assays measure the total cell cholesterol, so it is not possible to distinguish between plasma membrane cholesterol and intracellular cholesterol.

The total cell sphingomyelin ($\sim 10^4$ cells per assay) was estimated using the Amplex Red Sphingomyelinase Assay Kit (Molecular Probes). The level of the background (kit components without sphingomyelinase) did not allow measurements $<50\%$ total cell sphingomyelin; 0.03 U and 0.012 U/10,000 cells for 10 min in RPMI without serum decreases normal total cell sphingomyelin by $\geqslant 50\%$.

Cholesterol depletion

Cells were incubated in 10 mM β-CD (Sigma) (2×10^{-6} moles β-CD/10,000 cells) or with sphingomyelinase (Sigma; 0.03 U/10,000 cells) followed by 10 mM β-CD for the times indicated in the figures. β-CD was dissolved in supplemented RPMI 1640 medium either with or without 10% FCS at 37°C (Fig. S1, *B* and *C*, in Supplementary Material). Absence of FCS in the supplemented RPMI medium does not affect the total cell cholesterol levels for at least up to 4 h (data not shown). The same experiments were performed using 10 mM methyl β-cyclodextrin (mβ-CD), and the overall effect on the diffusion coefficients as a function of incubation time with mβ-CD is similar to the effect observed with β-CD. However, the plots level off earlier than those with β-CD (data not shown). For imaging, cells were labeled with Cy5-MCC 95-103 peptide before incubation with β-CD since the number of bound peptides per cell was too low if the cells were labeled after incubation with β-CD. This is not due to a reduced number of I-E^k present on the cell surface after β-CD treatment. The total number of native and GPI-linked I-E^k molecules, as evaluated by fluorescence-activated cell

sorting, using 14.4.4S antibody, is similar in β-CD-treated and untreated cells (data not shown). Therefore, we believe that the reduction in labeling efficiency is due to the MHC class II labeling mechanism. To bind peptide, MHC class II molecules need to be in an ''active'' form (Rabinowitz et al., 1998b). On the cell surface, the majority of active MHC class II molecules are recent arrivals from the endosomes (Vacchino and McConnell, 2001). If the membrane traffic between various cell organelles is halted due to the reduction of cholesterol concentration in the plasma membrane, no active MHC class II would be delivered to the surface. The reduction in labeling may also arise from cholesterol-mediated clustering of class II MHC molecules, which could lead to conformational changes in the peptide-binding groove or lower the rate of conversion from ''inactive'' to ''active'' class II MHC isomers. In addition, the labeling efficiency for the fluorescent lipid analogs ($DiIC_{12}$ and $DiIC_{18}$) also decreased after cholesterol depletion using sphingomyelinase followed by β-CD treatments. Cells were labeled with fluorescent lipid analogs before cholesterol depletion.

Addition of cholesterol

Cholesterol was added to either untreated cells or cells treated with β-CD. The concentration of chol-mβ-CD (Sigma) was adjusted to give 1 mM cholesterol (0.2×10^{-6} moles of cholesterol/10,000 cells). At this concentration, chol-mβ-CD is not fully soluble. A 0.1-mM chol-mβ-CD solution, which is soluble, produced the same results as a 1-mM solution, but over a longer time period (data not shown). Chol-mβ-CD was dissolved in supplemented RPMI 1640 with 10% FCS. Cells were incubated at 37°C for the times indicated in the figures (see Fig. 1, *B* and *C*, and Fig. S1 *A* and Fig. S2 in Supplementary Material). The solution above the cells was exchanged with a fresh one every 30 min. For the addition of cholesterol to the cholesterol-depleted cells, the cells were first incubated with 10 mM β-CD for 90 or 120 min and then incubated with chol-mβ-CD.

Labeling of primary amines

CHO-K1 cells were incubated with AlexaFluor647 NHS ester (Molecular Probes). Cells were labeled with 0.3–0.8 ng/μl Alexa (a stock solution at 2 μg/μl in dimethyl sulfoxide (DMSO)) for 20–30 min at 37°C in Hanks' balanced salt solution (Gibco BRL) supplemented with Na-pyruvate (Gibco BRL). These labeling conditions resulted in single-molecule labeling. Specifically, the fluorescent spots were 300–500 nm in diameter and separated by several microns. The intensity distribution of the fluorescent spots was not analyzed since it is very probable that certain classes of proteins will have more than one primary amine at the protein surface. Therefore, we did not distinguish between a single protein being labeled with multiple fluorophores and a cluster of proteins in which each protein is labeled with a single fluorophore and the whole cluster is $<$500 nm in diameter. The trajectories used in our analysis were obtained by recording the position, as a function of time, of the centers of fluorescent spots that were 300–500 nm in diameter and that exhibited blinking or bleached in one step. For experiments at reduced cholesterol levels, cells were labeled either before or after β-CD treatment. The order of labeling did not result in a significant difference in the measured diffusion coefficients (data not shown). The β-CD data presented in Fig. 5 contains trajectories from molecules labeled before β-CD treatment. We also labeled CHO-K1 cells with Cy5 NHS ester using the same protocol as for Alexa and achieved a labeling efficiency analogous to that of the Alexa case. However, the spectroscopic properties of Cy5 NHS ester attached to the proteins in this manner were different from that of Cy5 NHS ester attached to the antigenic peptide (e.g., the frequency of blinking was higher and the on time shorter).

FRAP—loading of lipid analog

For studies at normal and reduced cholesterol concentrations, the CHO-I-E^k cells were incubated with 0.5 μg/ml of $DiIC_{12}$ (stock 5 mg/ml in ethanol) for 20–30 min and 0.5 μg/ml of $DiIC_{18}$ (stock 1 mg/ml in ethanol) for 15 min at 37°C in supplemented RPMI 1640 media without FCS. For cholesterol reduction studies, cells were incubated with 10 mM β-CD in supplemented RPMI with 10% FCS for 120 min at 37°C or with 10 min sphingomyelinase (0.012 U/10,000 cells) followed by 10 mM β-CD for 10 min. For the β-CD studies, the cells were labeled with $DiIC_{18}$ and $DiIC_{12}$ after incubation with β-CD, whereas for the sphingomyelinase followed by β-CD studies, cells were labeled before sphingomyelinase treatment. Imaging was done at 22°C in supplemented RPMI without 10% FCS and either with or without enzymatic oxygen scavengers.

To verify that the enzymatic depletion of oxygen did not affect the rate of diffusion for membrane molecules the rate of diffusion for the $DiIC_{12}$ and $DiIC_{18}$ probes was measured with and without the presence of oxygen scavengers at the normal cholesterol level. The diffusion coefficient for the $DiIC_{12}$ probe in the presence of oxygen scavengers was $D = 1.47 \pm 0.81$ $\mu m^2/s$ (14 cells) and in the absence of oxygen scavengers was $D = 1.40 \pm 0.64$ $\mu m^2/s$ (nine cells). The diffusion coefficient for the $DiIC_{18}$ probe in the presence of oxygen scavengers was $D = 1.11 \pm 0.40$ $\mu m^2/s$ (10 cells) and $D = 1.01 \pm 0.42$ $\mu m^2/s$ (nine cells) and in the absence of oxygen scavengers was $D = 1.30 \pm 0.64$ $\mu m^2/s$ (11 cells) and $D = 0.97 \pm 0.70$ $\mu m^2/s$ (nine cells). Since the presence of oxygen scavengers did not affect the diffusion of these lipid analogs, we conclude that imaging under low oxygen levels

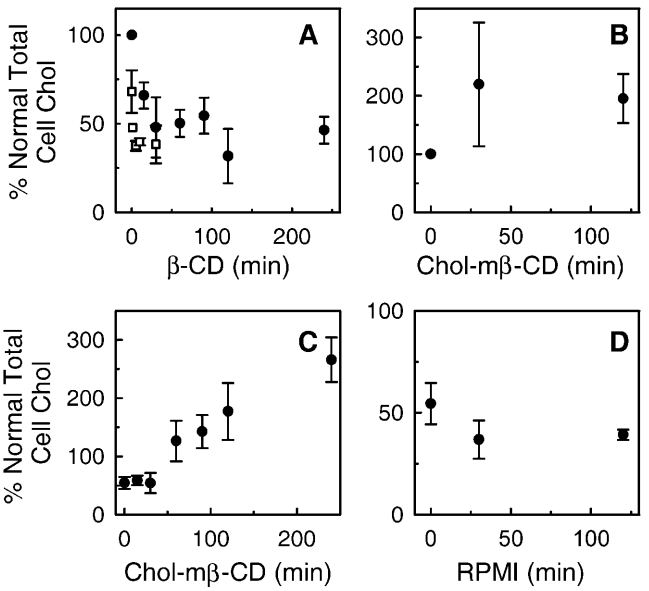

FIGURE 1 Modulation of cholesterol concentration. (*A*) Reduction in the percent of normal total cell cholesterol as a function of incubation time with β-CD. Cells were incubated with 10 mM β-CD (in RPMI with 10% FCS) (*closed circles*) or with 0.03 U sphingomyelinase for 10 min followed by 10 mM β-CD for the indicated times (*open squares*). Percent normal total cell cholesterol is defined as the ratio of total cell cholesterol in treated versus untreated cells for a particular condition averaged over at least four repeats. (*B*) Percent normal total cell cholesterol as a function of incubation time with 1 mM chol-mβ-CD. Cells not pretreated with β-CD were incubated with 1 mM chol-mβ-CD (in RPMI with 10% FCS) for the indicated times. (*C*) The percent normal total cell cholesterol as a function of incubation time with chol-mβ-CD after 90 min β-CD. First, cells were incubated with 10 mM β-CD (in RPMI 10% FCS) for 90 min at 37°C. Then β-CD was rinsed off ($t = 0$), and cells were incubated with 1 mM chol-mβ-CD (in RPMI, 10% FCS) for the indicated times. (*D*) Percent normal total cell cholesterol as a function of incubation time in RPMI (10% FCS) after β-CD treatment. Cells were treated with 90 min β-CD (in RPMI with 10% FCS), and at $t = 0$ min β-CD was rinsed off.

would not adversely affect the outcome of these experiments. The data presented in Table 1 include data taken with and without oxygen scavengers.

FRAP—experimental set-up and data analysis

FRAP measurements were performed using an inverted microscope (Eclipse TE300, Nikon, Burlingame, CA) with a 532-nm doubled Nd-YAG laser line (Millenia, Spectra-Physics, Mountain View, CA) for bleaching and monitoring of the probe. The epifluorescence was collected with a 100× magnification, 1.3 NA, oil-immersion objective (CFI PlanFluor) and imaged through a 545-nm dichroic mirror and 584-nm bandpass filter (Omega Optical, Brattleboro, VT). At the power used to monitor the fluorescence intensity, 20.0 ± 11.6 W/cm^2, photobleaching was negligible. An acousto-optic modulator (1205C-2, Isomet, Springfield, VA) was used to provide focused bleach pulses 200 ms in length (average half-width at 1/e^2 intensity = 0.98 ± 0.21 μm, average bleach power = 4.23 ± 2.71 kW/cm^2), resulting in an average percent bleach of 43.4 ± 12.2%. The fluorescence was imaged on an intensified frame-transfer CCD-camera (I-Pentamax, Roper Scientific, Trenton, NJ) with an acquisition rate of 10–20 Hz (region of interest: 60 × 60 pixels) or a Cascade 650 Si CCD-camera (Roper Scientific, Tucson, AZ). We used a nonlinear least-squares fit to the Brownian diffusion model described by Yguerabide et al. (1982) to obtain diffusion coefficients from the fluorescence recovery curves.

Cytoskeletal disruption

Stock solutions of nocodazole (Sigma; 20 mM stock) and cytochalasin D (Sigma; 1 mg/ml stock solution) were prepared in DMSO. Control cells were treated with an equivalent amount of DMSO alone. For tubulin depolymerization, cells were treated for 30 min at 37°C with 100 μM nocodazole (data not shown). For actin depolymerization, cells were treated for 30 min at 37°C with 40 μM cytochalasin D. Both drugs were present in the media during imaging. The effect of these drugs has been described elsewhere (Rotsch and Radmacher, 2000, Huby et al., 1998, Wakatsuki et al., 2000).

Experimental apparatus for single-molecule microscopy and analysis of the trajectories

The imaging conditions and diffusion analysis were performed as described in (Vrljic et al., 2002) with the following exception. Single-molecule trajectories were mapped by determining the center of the fluorescent spot in each frame with an accuracy of 53 nm, which represents the pixel size (in the previous report (Vrljic et al., 2002), the pixel size was incorrectly reported to be 60 nm). For single molecule studies images were collected at 10 Hz, 22°C.

Single Cy5 molecules adsorbed on a glass coverslip were imaged, and their position was determined with an accuracy of one pixel (53 nm). An immobile spot has a diameter of ~300 nm or ~6 pixels. A mobile spot has a diameter of ~500 nm or ~9 pixels. In the case of Figs. 2 and 3, all trajectories were clipped to have a length of 2.5 s (25 displacements, 100 ms per frame). The lowest observable diffusion coefficient for these data was then reported to be 2.8×10^{-4} μm^2/s ($D = \langle r^2 \rangle / 4t$, where $t = 2.5$ s, $r = 53$ nm). All diffusion coefficients reported were above the minimum detectable value as determined above.

TABLE 1 Diffusion of lipid probes

$DiIC_{12}$	% Immobile	D (μm^2/s)
Untreated	8.2 ± 7.3	1.2 ± 0.76
2 h β-CD	8.0 ± 5.2	0.63 ± 0.43
10 min SMase, 10 min β-CD	46.4 ± 21.0	0.53 ± 0.31
$DiIC_{18}$		
Untreated	7.8 ± 7.7	0.99 ± 0.60
2 h β-CD	8.5 ± 5.8	0.82 ± 0.43
10 min SMase, 10 min β-CD	33.9 ± 23.6	0.60 ± 0.59

Diffusion coefficients and percent immobile fraction were calculated from FRAP measurements. One recovery curve was measured per cell observed. $DiIC_{12}$: control, 30 cells; 120 min β-CD, 18 cells; 10 min sphingomyelinase followed by 10 min β-CD, 17 cells. $DiIC_{18}$: control, 40 cells; 120 min β-CD, 31 cells; 10 min sphingomyelinase followed by 10 min β-CD, 11 cells.

RESULTS

Lower cholesterol concentration correlates with lower diffusion coefficient

The cholesterol concentration was increased above normal (100%) by incubating cells with cholesterol-loaded mβ-CD (chol-mβ-CD) for up to 240 min (Fig. 1 *B*). The cholesterol concentration was reduced below normal by either incubating cells with β-CD or with sphingomyelinase followed by β-CD (Fig. 1 *A*). Previous studies suggest that β-CD preferentially extracts cholesterol over other lipids from the plasma membrane (Kilsdonk et al., 1995). Hydrolysis of sphingomyelin by sphingomyelinase facilitates removal of cholesterol by β-CD (Neufeld et al., 1996). The total cell cholesterol concentration gradually decreased as a function of incubation time with β-CD and leveled off at ~40% of the normal total cell cholesterol. We assume that most of the extracted cholesterol comes from the plasma membrane since that is the only cell surface in direct contact with β-CD. To assess reversibility of observed effects, cells treated with β-CD were then treated with chol-mβ-CD to replenish cholesterol (Fig. 1 *C*); the cells do not, on their own, replenish the extracted cholesterol over the time period of the experiments (Fig. 1 *D*). Cells were imaged in oxygen-depleted media, unless otherwise stated, at 22°C for up to 1 h, whereas treatments with different drugs before imaging were done at 37°C. Hypoxia had no effect on the diffusion of $DiIC_{12}$ and $DiIC_{18}$ probes (for details see Materials and Methods).

Although chol-mβ-CD treatment does not change cell morphology, β-CD treatment does change the cell morphology, with cells becoming slightly more rounded and less elongated than the untreated cells. The total number of native and GPI-linked I-E^k molecules is similar in untreated, β-CD-treated, and chol-mβ-CD-treated cells (data not shown). In addition, the number of I-E^k molecules labeled with Cy5 peptide per cell does not change after β-CD and chol-mβ-CD treatments (data not shown). We did not conclusively determine whether the surface area of the plasma membrane of the β-CD-treated cells is different than the surface area of the untreated cells. In addition, a small fraction of cells (after β-CD) displayed the morphology characteristic of late apoptosis as judged by transmission images and annexin V and propidium iodide staining (data not shown). Apoptotic

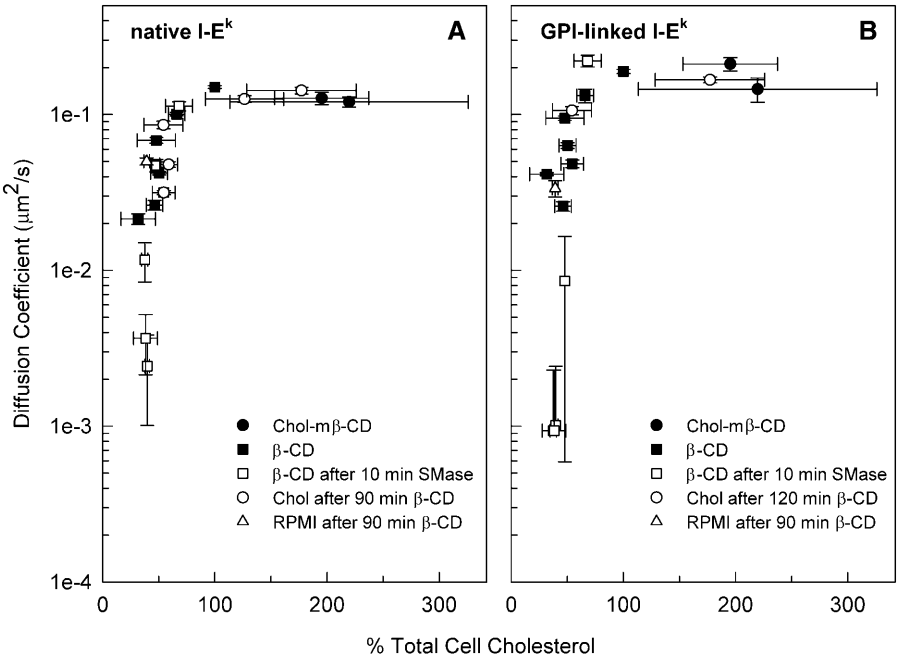

FIGURE 2 Diffusion coefficients as a function of cholesterol concentration. Diffusion coefficients calculated from fits to the cumulative distribution function averaged over all time lags (Vrljic et al., 2002) plotted against the corresponding percent normal total cell cholesterol value for (*A*) native I-E^k and (*B*) GPI-linked I-E^k. Cholesterol concentration was modulated as described in Fig. 1. For the number of trajectories contributing to each data point see Table S1 in Supplementary Material.

cells were not included in the analysis. Cells included in the analysis displayed a smooth plasma membrane (transmission image), and the staining patterns of annexin V and propidium iodide in these cells were comparable to the patterns seen in cells not treated with β-CD (data not shown).

The effect of varying the cholesterol concentration on the motion of GPI-linked and native I-E^k is shown in Fig. 2 and Figs. S1 and S2 in Supplementary Material. Single-molecule trajectories for the native and GPI-linked I-E^k proteins were used to calculate the diffusion coefficients, averaged over all time lags, at different cholesterol concentrations (see Table S1 in Supplementary Material for the number of trajectories and cells used in the analysis). At cholesterol concentrations above normal, the diffusion coefficients were similar to the diffusion coefficient at normal cholesterol (Fig. 2, *solid circles* and Fig. S1 *A* in Supplementary Material). The diffusion coefficients decreased by a factor of 5 for GPI-linked I-E^k and 7 for the native I-E^k when cholesterol was extracted using β-CD (Fig. 2, *solid squares* and Fig. S1, *B* and *C*, in Supplementary Material). The reduction of sphingomyelin concentration to $\leq$50% of normal (data not shown), by treatment with sphingomyelinase, caused a 30% decrease in normal cell cholesterol (Fig. 1 *A*) and a decrease in diffusion coefficient by a factor of 1.4 for the native I-E^k (Fig. 2 and Fig. S1 *E* in Supplementary Material). The same treatment did cause a 20% increase in the diffusion coefficient for the GPI-linked I-E^k (Fig. 2). The cholesterol concentration was reduced further by first treating the cells with sphingomyelinase and then incubating the cells with β-CD (Fig. 1 *A*, *open squares*). A 10-min sphingomyelinase treatment followed by β-CD treatment further reduced the diffusion coefficients by up to a factor of 60 for native and 190 for GPI-linked I-E^k (Figs. 2 (*open squares*) and S1 *E*). These molecules move 0–1 pixels (53 nm) in several seconds; thus the diffusion coefficients are below the detection limits of the camera and the diffusion coefficient is reported as the resolution limit, 2.8×10^{-4} μm^2/s.

It is interesting to note that although the change in cholesterol concentration between 120 min β-CD and 10 min sphingomyelinase followed by 10 min β-CD is biochemically undetectable with our assay (Fig.1 *A*), the diffusion behavior of both proteins is very different after the treatments. We believe that this effect is due to very small changes in the cholesterol concentration (undetectable using our assay) based on the following arguments. First, in the case of the native I-E^k, after the sphingomyelin concentration is reduced to $\leq$50% of the total normal cell sphingomyelin concentration, the total cell cholesterol was measured to be 68% of normal and the diffusion coefficient matches the diffusion coefficient observed after 15 min β-CD where the cholesterol concentration is reduced to 65% of total normal (Fig. 1 *A* and Fig. S1 *E* in Supplementary Material). Second, reduction of sphingomyelin concentration facilitates extraction of cholesterol by β-CD (Fig. 1 *A*, and Neufeld et al., 1996). Third, this decrease in diffusion coefficient is reversible upon addition of cholesterol without addition of sphingomyelin (see below). Cholesterol may fluidize an otherwise solid-like ceramide membrane.

The two striking features of Fig. 2 are the large decrease in diffusion coefficients, by up to a factor of 60 for native and 190 for GPI-linked I-E^k, and the rate of change of the diffusion coefficient as a function of cholesterol concentration. The rate is different for cholesterol concentrations above and below normal cholesterol concentration. A small

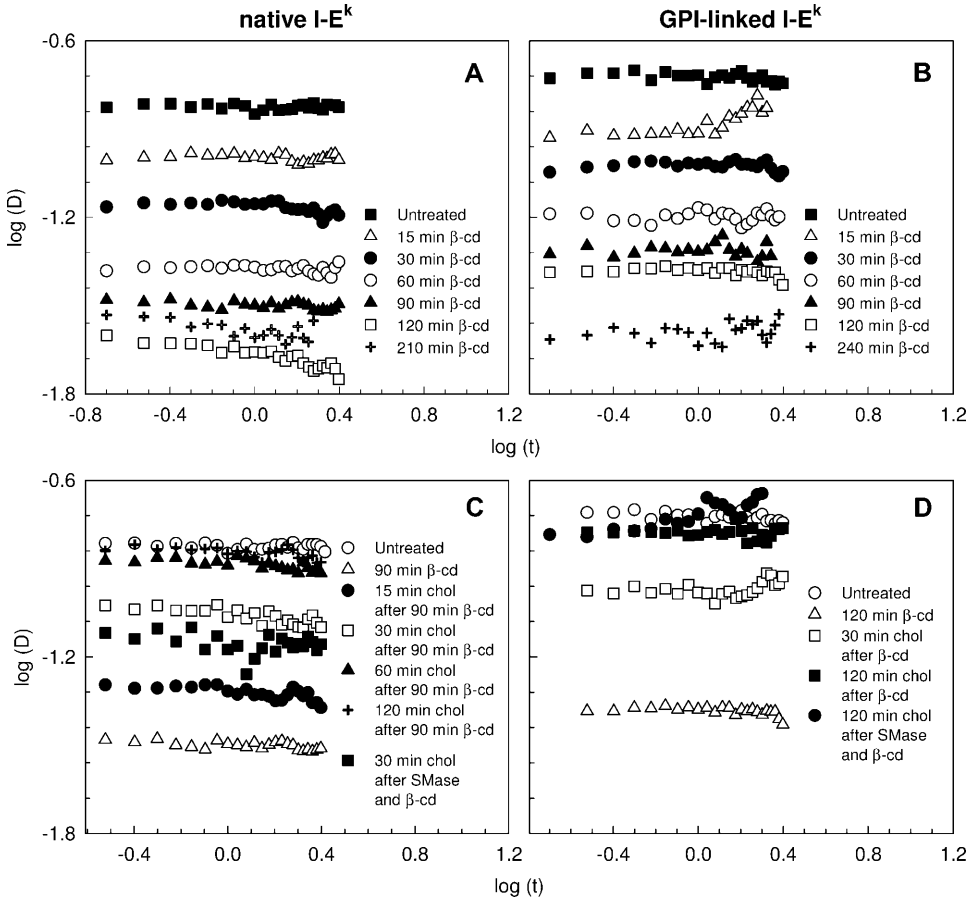

FIGURE 3 Diffusion coefficients at different cholesterol concentrations. Log of diffusion coefficients for cholesterol extraction calculated from fits to the cumulative distribution function (Vrljic et al., 2002). 50-200 trajectories contribute to each time lag (for details, see Supplementary Material). Time resolution is 100 ms per frame. (*A*) Native I-E^k after different incubation times with β-CD (see Fig. 1 *A* for the corresponding values of total cell cholesterol). (*B*) GPI-linked I-E^k, conditions as in *A*. (*C*) Native I-E^k after different incubation times with chol-mβ-CD on cells pretreated with 90 min β-CD (see Fig. 1 *C* for the corresponding levels of cholesterol). The untreated (*open circles*), 90 min β-CD (*open triangles*), and 10 min sphingomyelinase (SMase) followed by 10 min β-CD and then 30 min chol-mβ-CD (*closed squares*) data are shown for comparison. (*D*) GPI-linked I-E^k after different incubation times with chol-mβ-CD on cells pretreated with 120 min β-CD. The untreated (*open circles*), 120 min β-CD (*open triangles*), and 10 min sphingomyelinase followed by 10 min β-CD and then 2 h chol-mβ-CD (*filled circles*) data are shown for comparison.

or negligible change in diffusion coefficients is observed at cholesterol concentrations above normal, and a large decrease occurs at cholesterol concentrations below normal. We believe that this large drop in diffusion at the lower cholesterol concentrations is related to cholesterol-phospholipid interactions. That is, it has been known for some time that phospholipid in a solid-like state can be converted to a fluid state on addition of cholesterol (Feingold, 1993). As discussed later, we think this ''fluidization'' is due to the formation of liquid complexes of cholesterol and phospholipid. Extraction of cholesterol from the plasma membrane can then reverse a process of this sort when there are high-temperature melting phospholipids in the plasma membrane. See Discussion.

Cholesterol reintroduction restores protein motion

Cholesterol was reintroduced to the cholesterol-depleted cells by incubating with chol-mβ-CD after a 90- or 120-min β-CD treatment (Fig. 1 *C*). Since our cholesterol assay measures the total cell cholesterol, we cannot be certain that the plasma membrane cholesterol reaches 250%. After this treatment the morphology of the cells did not change compared to the cells treated with β-CD for 120 min (data not shown). The number of fluorophores per cell as well as the total number of native and GPI-linked I-E^k molecules per cell did not change relative to the untreated and β-CD-treated cells (data not shown).

Fig. 2, *A* and *B* (*open circles*), and Fig. S2 in Supplementary Material, show that the diffusion coefficients increase as cholesterol is reintroduced to the cells and level off at the value of the diffusion coefficient of untreated cells. The motion of I-E^k proteins in the sphingomyelinase-treated cells also increases (Fig. 3 *C*) and fully recovers (Fig. 3 *D*) after addition of cholesterol, demonstrating that the decrease in motion was due to the loss of cholesterol, not sphingomyelin. The diffusion coefficients at any particular cholesterol concentration are similar regardless of the drug treatment, suggesting that the effect is dependent on the cholesterol concentration and independent of the treatment history.

Recovery of diffusion was only observed after the reintroduction of cholesterol. Neither the total cell cholesterol levels nor the motion of native and GPI-linked I-E^k proteins change for at least 120 min after β-CD-mediated cholesterol depletion (Fig. 1 *D* and Fig. 2, *open triangles* and Fig. S1 *F* in Supplementary Material), suggesting that intracellular cholesterol ester stores, metabolic production of cholesterol, and cholesterol flux from the media do not change the total

cell cholesterol concentration for up to 120 min after β-CD treatment. Redistribution of cholesterol between intracellular cholesterol pools, intracellular membranes, and plasma membranes is insufficient to mediate full recovery of the diffusion coefficients of native and GPI-linked I-E^k proteins.

After incubation with supplemented RPMI media for up to 120 min after β-CD, the cell morphology did not change compared to the β-CD-treated cells (data not shown). The number of fluorophores per cell as well as the total number of native and GPI-linked I-E^k molecules per cell did not change compared to the β-CD-treated cells (data not shown). However, after incubation with supplemented RPMI media for 20 h after a 3-h β-CD treatment, the cell morphology changed to resemble that of the untreated cells. The cells stretched and readhered to the surface. In addition, cells proliferated, indicating that the long-term viability of the cells treated for 3 h with β-CD was not compromised (data not shown).

Protein diffusion is Brownian on a 100-ms timescale

Diffusion coefficients for the native and GPI-linked I-E^k proteins at different cholesterol concentrations were examined as a function of time lags between $t = 0.1$ and 2.5 s to determine if the motion was Brownian at reduced cholesterol levels (Fig. 3). Diffusion coefficients appear to deviate from Brownian motion at time lags longer than 2.5 s (data not shown) due to averaging of data with different trajectory lengths and diffusion coefficients from different imaging sessions. The largest observed variation of diffusion coefficients from different imaging sessions is 20%. Trajectory lengths were clipped to match the shortest lengths from different imaging sessions (2.5 s).

Deviation from ideal Brownian motion has been characterized by the anomalous diffusion parameter, α. For two-dimensional Brownian motion $\alpha = 1$ and for anomalous diffusion $0 < \alpha < 1$ ($D = D_0 t^{\alpha-1}$; $\langle r^2 \rangle = 4D_0 t^{\alpha}$ (Smith et al., 1999; Saxton, 1994; Feder et al., 1996). At all cholesterol levels, the α parameters for both GPI-linked and native I-E^k have values close to one, indicating that the diffusion is Brownian for time lags up to 2.5 s (see Tables S2 and S3 in Supplementary Material) when imaged at 10 Hz.

Population is homogeneous at all cholesterol levels

Since the analysis of diffusion coefficients presented up to this point disregards the individuality of the trajectories, distributions of apparent diffusion coefficients were constructed from individual trajectories at different cholesterol concentrations to probe for heterogeneity (Fig. 4). The lines plotted over the histograms are not fits, but the probability distribution of apparent diffusion coefficients expected for a single population, taking into account finite trajectory length (Eq. A1 from Vrljic et al., 2002). The arithmetic mean of D_es from all trajectories, at a time lag of 0.2 s, was used as an estimate for the underlying true D_0.

Multiple, distinct populations are not obvious from the distributions of apparent individual diffusion coefficients for GPI-linked I-E^k when the time resolution is 100 ms. As cholesterol is depleted, the entire population gradually narrows and shifts toward a distribution with a lower D_0 (compare panel *F* of Fig. 4 with panels *A*– *C*). Upon cholesterol reintroduction (compare Fig. 4 *A* with Fig. 4, *D* and *E*), the distribution gradually shifts back toward a higher D_0. After 120 min of cholesterol reintroduction, the distribution of apparent individual diffusion coefficients is similar to the distribution for untreated cells (compare panels *E* and *F* of Fig. 4). Addition of cholesterol to untreated cells causes a slight increase in D_0 (compare panels *F* and *H* of Fig. 4). The distributions of the apparent individual diffusion coefficients for the native I-E^k molecules, at all cholesterol concentrations, were similar to the distributions shown for the GPI-linked I-E^k molecules (data not shown).

The distributions of apparent individual diffusion coefficients for GPI-linked I-E^k at all cholesterol concentrations are slightly broader than the expected distribution for a population of diffusers with a single diffusion coefficient, suggesting the potential presence of multiple populations or a small deviation from Brownian motion.

Diffusion of other membrane components also depends on cholesterol concentration

Primary amines on the surface of CHO-K1 cells (not transfected with I-E^k molecules) were labeled with low concentrations of the AlexaFluor647 NHS ester fluorophore. NHS ester reacts with primary amines on proteins or phosphatidylethanolamine (PE). Since PE is enriched in the cytoplasmic leaflet of the plasma membrane, we expected the probability of labeling proteins in the extracytoplasmic leaflet to be higher than the probability of labeling PE. The distribution of individual apparent diffusion coefficients for AlexaFluor647 NHS ester-labeled proteins and PE at normal cholesterol concentration (Fig. 5 *A*) is broader than expected for a homogenous, single population of diffusers (theoretical plot not shown). This difference is expected since the labeling method employed can label single-pass, multipass, and lipid-linked membrane proteins, as well as oligomerized proteins and lipids (PE). Since the recently reported diffusion coefficients of single-fluorophore-labeled lipids (at 37°C) are very similar to reported protein diffusion coefficients (Schütz et al., 2000; Fujiwara et al., 2002; Murase et al., 2004; Vrljic et al., 2002; Kenworthy et al., 2004), the observed diffusion coefficients for AlexaFluor647-labeled membrane components (0.01–0.3 $\mu m^2/s$) suggest that membrane proteins or lipids could have been labeled by this method. The average of individual diffusion coefficients at ~30% of normal total cell cholesterol (90 min β-CD) (*crosshatched bars*) is much

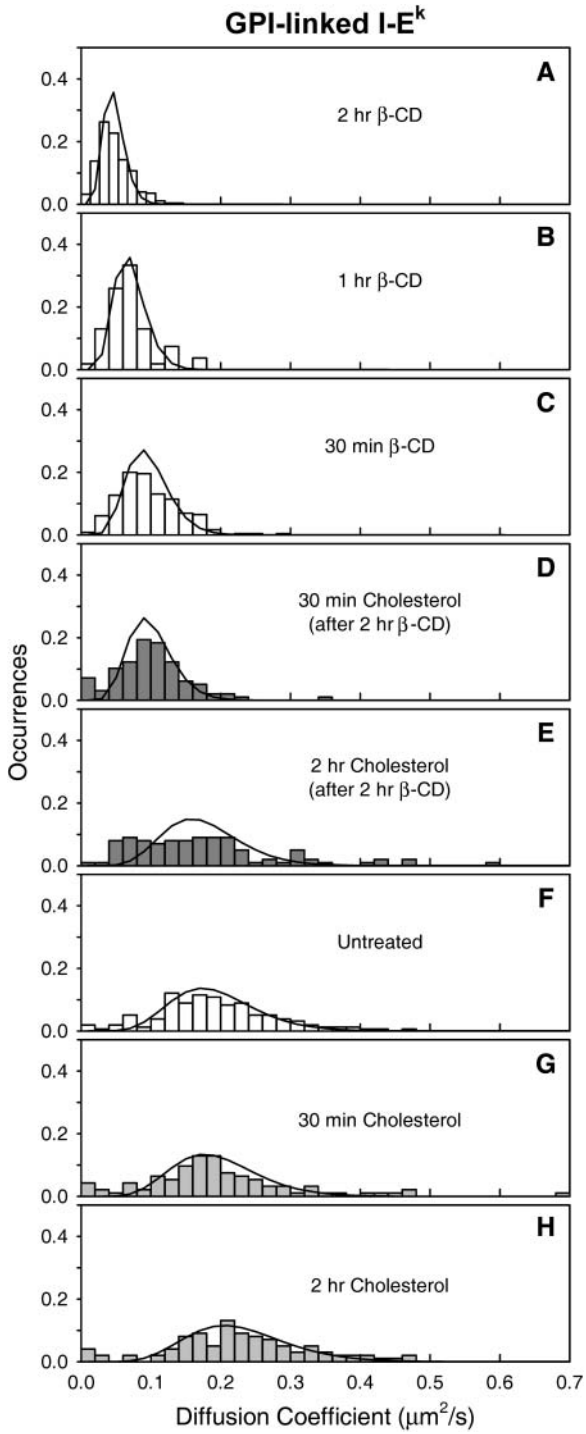

FIGURE 4 Distribution of apparent diffusion coefficients of individual trajectories. GPI-linked I-E^k diffusion coefficients for individual trajectories were estimated as described in Vrljic et al. (2002) and used to build a histogram of apparent diffusion coefficients for a time lag of 0.2 s. Trajectories that lasted ≥2.1 s were clipped to be 2.1 s long. The time lag (0.2 s) was chosen such that 10 displacements from each trajectory were used to calculate diffusion coefficient, D_e ($N = 10$). The solid line represents the expected distribution of diffusion coefficients for a homogeneous population of Brownian diffusers (Vrljic et al., 2002). (*A*) 120 min β-CD, 266 trajectories, $\langle D_0 \rangle = 0.048 \pm 0.018\ \mu m^2/s$. (*B*) 60 min β-CD, 54 trajectories, $\langle D_0 \rangle = 0.060 \pm 0.021\ \mu m^2/s$. (*C*) 30 min β-CD, 245 trajectories, $\langle D_0 \rangle = 0.081 \pm 0.037\ \mu m^2/s$. (*D*) 30 min chol-mβ-CD after 120 min β-CD, 98 trajectories, $\langle D_0 \rangle = 0.082 \pm 0.036\ \mu m^2/s$. (*E*) 2 h chol-mβ-CD after 120 min β-CD, 100 trajectories, $\langle D_0 \rangle = 0.13 \pm 0.075\ \mu m^2/s$. (*F*) Untreated, 157 trajectories, $\langle D_0 \rangle = 0.14 \pm 0.073\ \mu m^2/s$. (*G*) 30 min chol-mβ-CD, 93 trajectories, $\langle D_0 \rangle = 0.14 \pm 0.079\ \mu m^2/s$. (*H*) 2 h chol-mβ-CD, 99 trajectories, $\langle D_0 \rangle = 0.17 \pm 0.95\ \mu m^2/s$.

lower than the average at normal cholesterol concentration (*gray bars*). The reduction of diffusion coefficients is reversible upon addition of cholesterol (*white bars*) and matches the distribution for the untreated cells. Surface levels of labeled protein(s) do not appear to change upon treatment with β-CD or chol-mβ-CD based on the observed labeling efficiency. Also, the number of fluorophores per cell was similar regardless of whether the cells were labeled before or after β-CD treatment (data not shown).

To determine if the motion of the labeled molecules conforms to two-dimensional Brownian motion, the diffusion coefficients at different cholesterol concentrations were examined as a function of time lag. Plots in Fig. 5 *B* indicate that the motion of the labeled protein(s) is predominantly Brownian at all studied cholesterol concentrations when imaged at 10 Hz. The motion of the labeled protein(s) was not affected by cytochalasin D and nocodazole (data not shown). These results closely mimic the behavior of the class II MHC proteins described above.

Lipid analogs show cholesterol-mediated changes in diffusion

The diffusion coefficients of two lipid analogs, $DiIC_{12}$ and $DiIC_{18}$, were measured by FRAP at 100% and 30–40% of normal total cell cholesterol (0, 120 min incubation with β-CD, and 10 min sphingomyelinase followed by 10 min β-CD). See Fig. S3 in Supplementary Material for a representative FRAP recovery curve for $DiIC_{12}$ after 120 min β-CD treatment. The recovery curves were fit well assuming nonanomalous diffusion (Yguerabide et al., 1982) suggesting that the diffusion of $DiIC_{18}$ and $DiIC_{12}$ is predominately Brownian at all studied cholesterol concentrations when imaged at 10 Hz and 20 Hz.

Table 1 shows the diffusion coefficients and percent immobile fraction for both fluorescent lipid analogs at different cholesterol concentrations. Although the diffusion coefficients for both lipid analogs decrease slightly after cholesterol extraction (at most a factor of ~2), the percent immobile fraction increased from 8% to 30–50% after cholesterol extraction and sphingomyelinase treatment. Analogous to the behavior of GPI-linked and native I-E^k, the change in cholesterol concentration between the 120-min β-CD treatment and the 10-min sphingomyelinase followed by 10-min β-CD treatment is biochemically undetectable (Fig.1 *A*), but the diffusion behavior for the lipid probes is very different at these cholesterol concentrations.

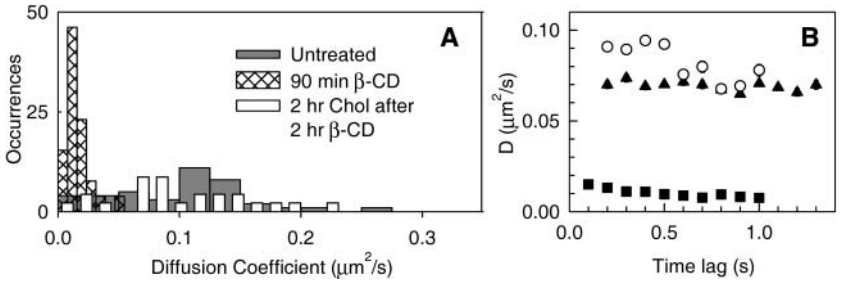

FIGURE 5 Protein(s) on CHO K1 plasma membrane labeled with AlexaFluor 647 NHS ester. (*A*) Distribution of diffusion coefficients for individual Alexa 647-labeled protein(s) at a time lag of 0.2 s. Untreated, 40 trajectories; 90 min β-CD, 26 trajectories; and 120 min β-CD followed by 120 min chol-loaded β-CD, 24 trajectories. (*B*) Diffusion coefficients for Alexa 647-labeled protein(s) at different cholesterol levels. Open circles: untreated, 55 trajectories, 13 cells, max t_{lag} 1.3 s, $\alpha = 0.97 \pm 0.02$; filled squares: 90 min β-CD (labeled before treatment), 49 trajectories, nine cells, max t_{lag} (49 tracks contribute) 1.0 s, $\alpha = 0.68 \pm 0.05$; filled triangles: 120 min β-CD followed by 120 min chol-loaded β-CD, 57 trajectories, six cells, max t_{lag} 1.0 s, $\alpha = 0.82 \pm 0.06$. The maximum time lag is defined as the longest time lag at which at least 50 trajectories contribute. In cases with fewer than 50 trajectories, the maximum time lag is the length of the shortest trajectory.

Changes not due to actin cytoskeleton

Previously we showed that perturbation of the actin cytoskeleton using cytochalasin D had no major effect on the motion of the native and GPI-linked I-E^k at a normal cholesterol concentration (Vrljic et al., 2002). Cells incubated with β-CD exhibit morphological changes (become more spherical) indicative of actin cytoskeletal rearrangements through the loss of adhesion points, thus suggesting the possibility that the observed decrease in the diffusion coefficients may be due to rearrangement of the actin cytoskeleton.

Cells at a reduced cholesterol concentration (120-min incubation with β-CD) were treated with cytochalasin D. The morphology of cells treated with cytochalasin D changed to become less elongated than those cells treated with only β-CD, suggesting that the drug had an effect on the actin cytoskeleton (data not shown).

The diffusion coefficients extracted from time lags up to 2.5 s were used to analyze the motion of native and GPI-linked I-E^k in cholesterol-depleted cells treated with cytochalasin D (Fig. 6, *A* and *B*). The diffusion coefficients and overall shape of the plots before and after treatment with cytochalasin D are similar and α parameters are close to one (see Tables S1 and S2 in Supplementary Material). These results suggest that the observed decrease in the diffusion coefficients upon cholesterol extraction is probably not due to changes in the actin cytoskeleton. The role of the tubulin network in the decrease of diffusion coefficients was addressed by incubating cells with nocodazole. Treatment with nocodazole also had no effect on the diffusion coefficients at normal (Vrljic et al., 2002) and reduced cholesterol concentrations (data not shown).

DISCUSSION

In this work, we determined that the diffusion coefficients of native I-E^k, GPI-linked I-E^k, other protein(s), and fluorescent lipid analogs $DiIC_{18}$ and $DiIC_{12}$ decrease as a function of plasma membrane cholesterol concentration. The decrease in the diffusion coefficients correlates with a decrease in the total cell cholesterol concentration, with the diffusion coefficients decreasing by up to a factor of 7 for native and 5 for GPI-linked I-E^k. At low cholesterol concentrations, after sphingomyelinase treatment, the diffusion coefficients are reduced by up to a factor of 60 for native and 190 for GPI-linked I-E^k (Fig. 2). Although the diffusion coefficients for the lipid analogs do not decrease nearly as much as those of the proteins, the percent immobile fraction of the lipid analogs does significantly increase at a lower cholesterol concentration and sphingomyelinase treatment. At label concentrations higher than the single-molecule labeling level, the spatial distributions of fluorescently labeled native and GPI-linked I-E^k at normal and reduced cholesterol concentrations appear uniform (data not shown). This observation is consistent with the results reported for GM1 and GPI-linked proteins (Kenworthy et al., 2000; Hao et al., 2001).

We speculate, for several reasons, that most of the cholesterol being extracted comes from the plasma membrane. First, it has been reported that 65–90% of the total cell unesterified cholesterol is present in the plasma membrane (Warnock et al., 1993; Lange, 1991). Secondly, cyclodex-

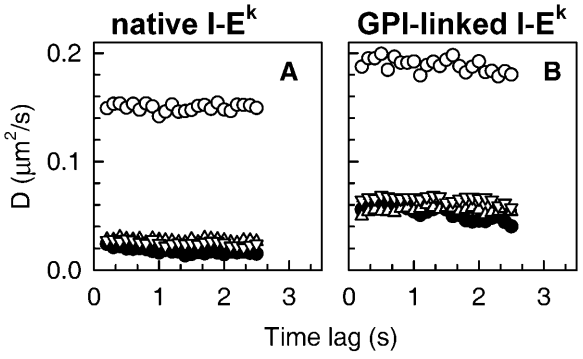

FIGURE 6 Influence of actin cytoskeleton. (*A*) Diffusion coefficients versus time lag for native I-E^k after (●) 120 min incubation with β-CD followed by 30 min cytochalasin D treatment; (▽) 120 min β-CD followed by DMSO; (△) 120 min β-CD. Untreated case (○) plotted as a reference (see Fig. 2 *A* for details). (*B*) GPI-linked I-E^k: (●) 120 min incubation with β-CD followed by 30 min cytochalasin D; (▽) 120 min β-CD followed by DMSO; (△) 120 min β-CD. Untreated case (○) plotted as a reference (see Fig. 2 *B* for details). See Supplementary Material for the number of trajectories contributing to each data point.

trin-mediated cholesterol efflux from the plasma membrane is biphasic (Kilsdonk et al., 1995; Haynes et al., 2000; Steck et al., 2002). (In our work, the fast-phase rate estimated from Fig. 1 *A* is 10^{-2} min^{-1}/mM β-CD, about a factor of 10 less than that observed for monolayer mixtures (Radhakrishnan and McConnell, 2000a)). Haynes et al. (2000) proposed that the kinetic profile of cholesterol extraction is due to the presence of different kinetic pools of cholesterol in the plasma membrane rather than intracellular stores, which is consistent with our finding (compare Fig. 1 and later discussion). The observed decrease in the lateral diffusion for the proteins studied herein reflects their high sensitivity to the changes in plasma membrane composition.

The decrease in diffusion of the tested proteins after cholesterol extraction is reversible upon reintroduction of cholesterol. This is consistent with the biochemical finding by Huby et al. (1999), who observed that the inhibitory effect of mβ-CD on HLA-DR signaling in THP-1 cells is reversible upon incubation with chol-mβ-CD. Although Huby et al. (1999) have observed inhibition of tyrosine phosphorylation upon excessive loading with cholesterol, we did not observe a significant change in the diffusion upon addition of cholesterol to the cells with normal cholesterol concentration (for up to 2 h chol-mβ-CD).

Cells were incubated for times >120 min with β-CD, but it did not appear that the percent of normal total cell cholesterol decreased to <30%. Protein diffusion did not change further after incubation of up to 6 h with β-CD (data not shown). In apoptotic cells, protein diffusion was observed to be faster than at normal cholesterol levels (the diffusion rate was above the resolution limit of the detector). The protein motion was found to be fast in cells induced to undergo apoptosis after extensive β-CD treatment and in cells treated with staurosporine A without β-CD treatment (data not shown), suggesting that the effect is independent of specific β-CD effects. It is unclear if this effect is mediated by loss of lipid asymmetry, changes in lipid composition of the membrane, or cytoskeletal rearrangements different from those induced by cytochalasin D and nocodazole treatments.

The effect of cholesterol depletion on diffusion was reported for two cholesterol points (normal and reduced) at 37°C by Kenworthy et al. (2004). In this work, we report on the diffusion coefficients for a large range of cholesterol concentrations and are able to observe the nonlinear rate of change in the diffusion coefficients that occurs between ~40–50% and 200% total cell cholesterol at 22°C. Also, we demonstrate that the effect we see is cholesterol-mediated in that cholesterol repletion restores the motion of the proteins.

Since cells do change shape after cholesterol depletion, we considered the possibility that the decrease in protein diffusion coefficients was caused by rearrangement of the cellular cytoskeleton. Contrary to the observation by Kwik et al. (2003), at similar cholesterol concentrations, cytochalasin D and nocodazole treatment after cholesterol depletion did not affect the diffusion of the native I-E^k, GPI-linked I-E^k (Fig. 6, and data not shown) and Alexa647-labeled protein(s) (data not shown). Also, again contrary to the results found by Kwik et al. (2003), addition of cholesterol to cholesterol-depleted cells does not change the cell morphology within 2 h, but does change the value of the diffusion coefficients. Thus the effect observed in this study is not likely to be mediated by PIP 2-actin system.

The discrepancy between these observations may be due to the differences in imaging temperatures, exact conditions of the cytochalasin D treatments, and the hypoxic conditions used during imaging in the current study. As discussed by Murakoshi et al. (2004), the effect of different concentrations of actin-depolymerizing drugs on diffusion is not straightforward. At low concentrations, cytochalasin D is reported to inhibit actin polymerization, whereas at higher concentrations Murakoshi et al. (2004) report that cytochalasin D induces actin aggregation.

In the current literature there are conflicting reports on the effect of hypoxia on the actin cytoskeleton (Daniliuc et al., 2003; Su et al., 2003; Alsat et al., 1996; Nurko et al., 1996). Some groups report that hypoxic conditions may induce rearrangement of the actin cytoskeleton, but in these experiments the hypoxic conditions were attained by culturing the cells in anaerobic chambers for 24–72 h. Since peroxides are known byproducts of anaerobic metabolism, and it is unclear whether cells were able to neutralize the peroxides without the addition of peroxide scavengers, it is possible that the reported actin rearrangement was actually induced by a combination of peroxide damage and oxygen depletion. In our experiments we have tried to minimize peroxide damage to the cells by using catalase and β-mercaptoethanol in the enzymatic oxygen scavenger system.

There are two possible effects on molecular motion in membranes resulting from changes in cholesterol concentration: changes to the Brownian character of the diffusion and changes in the value of the diffusion coefficient. There is an extensive theoretical literature on subtle effects of immobile and mobile obstacles, as well as confinements (Qian et al., 1991; Saxton, 1990, 1992, 1993, 1994, 1995, 1997). For the protein to show confined behavior, the confining domain needs to be relatively immobile with respect to the protein, and the protein needs to spend a large fraction of time within the domain. The motion of proteins (for up to 2.5 s, $\Delta t = 100$ ms) and lipid analogs in our study were Brownian for all cholesterol concentrations (Fig. 3) when imaged at 10 Hz or 20 Hz, thus ruling out the presence of stable, immobile domains having radii of up to ~1.3 μm at normal and ~0.4 μm at ~30–50% of normal total cell cholesterol (based on $\langle r^2 \rangle = 4Dt$, $t = 2.5$ s). Our results do not exclude immobile domains with radii larger than ~1.3 μm at normal cholesterol and ~0.4 μm at 30–50% of normal total cell cholesterol, mobile domains, unstable domains, or domains with permeable boundaries.

Our results are consistent with the predominantly Brownian diffusion of Cy3- di-oleoylphosphatidylethanol-

amine (DOPE) in the plasma membrane of various cell types (Fujiwara et al., 2002; Murase et al., 2004) when observed with an imaging rate of 100 ms per frame. Fujiwara et al. (2002) and Murase et al. (2004) report that the diffusion of DOPE-labeled with 40 nm gold beads was anomalous when continuously imaged at a rate of 25 μs/frame. In particular, 32 nm actin-mediated compartments were reported in CHO cells when DOPE-gold was observed at a rate of 25 μs per frame (Murase et al., 2004). The results of our study do not exclude the existence of these actin-mediated barriers to membrane diffusion, and given the results of Fujiwara et al. and Murase et al., it is unlikely we would observe them using an imaging rate of 10 Hz.

The observed changes in the values of protein diffusion coefficients can also be discussed in terms of a model of two-dimensional Brownian motion in membranes. This model was originally described by Saffman and Delbruck (1975; SD) and extended by Hughes, Pailthorpe, and White (1981; HPW) (Hughes et al., 1981). The SDHPW model describes the motion of a rigid cylinder with a given radius in a two-dimensional liquid with a given thickness and viscosity surrounded in the third dimension by liquids with distinct viscosities. Although this model is highly idealized, it is useful to provide perspective on the implications of our observations (for a detailed discussion of the model see Supplementary Material). We find that the observed decrease in the protein diffusion coefficients cannot be accounted for by plausible changes in membrane viscosity or effective radius of the diffuser. According to the SDHPW calculation, the effective viscosities experienced by the DiI lipid analogs and the native and GPI-linked I-E^k proteins at different cholesterol concentrations need to be very different if the diffusers are assigned radii consistent with known molecular structures. Moreover, the observed diffusion coefficients require the viscosity of the membrane to increase to ~3000–18,000 Poise after cholesterol extraction. Otherwise the radius of the diffusing object would need to increase to ~100 μm (see Table S4 and text in Supplementary Material). Clearly, no plausible contortions of a simple fluid mechanics model can be used to describe the experimental results.

Some insight into the effect of cholesterol concentration on diffusion is provided by studies of model membranes. For example, in binary mixtures of dimyristoylphosphatidylcholine (DMPC) and cholesterol (Smith et al., 1980), the lateral diffusion of a phospholipid probe decreases sharply (by a factor of ~10) as the cholesterol concentration is decreased to <20%, when the temperature is below the chain-melting temperature of the pure phospholipid. This same result holds for the diffusion of the M-13 coat protein incorporated in DMPC/Chol bilayers at temperatures below the chain-melting temperature, with the diffusion coefficient decreasing by a factor of ~100. However, at temperatures above the chain-melting temperature for DMPC the diffusion coefficient has a minimum at ~25 mol % cholesterol (Smith et al., 1980; Almeida et al., 1992), and the maximum decrease in the diffusion coefficient is ~3 (Smith et al., 1980). If we simply extrapolate these results to cell membranes, we can anticipate the possibility of larger effects of cholesterol extraction on diffusion at lower temperatures.

We believe that these diffusion data as well as other physical properties of binary mixtures of cholesterol and phospholipids in monolayer and bilayer mixtures can be understood in terms of liquid ''condensed complexes'' (Radhakrishnan and McConnell, 1999; McConnell and Radhakrishnan, 2003). The basic idea is that for every phospholipid, there is a reversible reaction with cholesterol for which one can assign an equilibrium constant and a stoichiometry. The addition of cholesterol to a reactive phospholipid membrane is then somewhat like a strong acid-base pH titration. At the equivalence point the activity of both protons and hydroxide are low, whereas on the acidic and basic sides of the equivalence point the activities of protons and hydroxide groups are large and small, and small and large, respectively. In cholesterol titration into a phospholipid bilayer, the cholesterol activity remains low until the equivalence point is passed, after which it increases until it equals that of solid cholesterol, at which point solid cholesterol is formed. As cholesterol is lowered below the equivalence point, the activity of phospholipid increases. The phospholipid activity may then increase until it equals that of solid phospholipid at lower temperatures, in which case solid phospholipid forms. The above results on the diffusion of probes in DMPC/Chol bilayers are consistent with this model. Assuming the stoichiometry for this system is ~20% cholesterol, the minimum in the diffusion of M-13 and a lipid probe occurs when the complex concentration is a maximum. In the case where the temperature is below the DMPC melting temperature, and the cholesterol concentration is below the stoichiometric composition, there is a precipitous drop in the diffusion coefficient since the free phospholipid freezes. It is possible that cholesterol forms similar liquid complexes with ceramides.

We make a two-step extrapolation of this picture of complexes to our results on the plasma membrane of CHO cells. The first step is to the complex mixture of lipids in the plasma membrane. In the earlier monolayer studies of cholesterol-phospholipid mixtures, a number of physical properties of these mixtures undergo abrupt changes as one changes cholesterol concentration from below stoichiometric (excess phospholipid) to above stoichiometric (excess cholesterol). Although this switch in properties has been seen with ternary mixtures of phospholipids and cholesterol in monolayers, it has not yet been demonstrated with the complex mixtures found in plasma membranes. (For ternary or more complex mixtures the term ''equivalence composition'' is preferred over ''stoichiometric composition''.) In our first step we assume that there is a cholesterol-dependent jump in the physical properties of membrane lipids as a function of cholesterol concentration.

There is now substantial evidence that the biochemical properties of the plasma membranes of cells do change sharply as a function of cholesterol concentration, around the ''normal'' concentration (Lange et al., 2004; Sooksawate and Simmonds, 2001). The second step in our extrapolation is then to assume that the normal cholesterol concentration in plasma membranes is the equivalence composition referred to above. The drop-off in diffusion we observe at cholesterol concentrations below normal is then attributed to the formation of excess phospholipid (and sometimes ceramide) under these circumstances. That is, the experimental temperature of 22°C is presumed to be below the freezing temperature of a number of these lipids, leading to a reduction in diffusion analogous to that discussed above in connection with DMPC/Chol mixtures.

In model membranes, Radhakrishnan and McConnell (2000b) have shown that changes in electrical potential across a membrane can lead to changes in the phase state of the lipid monolayer. Transmembrane potentials in cells are on the order of 100 mV/10 Å, and transmembrane voltage drops of this magnitude could lead to electrostriction. The effect of membrane depolarization on the diffusion coefficients for the native and GPI-linked I-E^k proteins has been explored (see Fig. S4 and text in Supplemental Material).

Our proposals above are consistent with observations of Hao et al. (2001) and Kenworthy et al. (2004). Hao et al. observed a uniform fluorescence intensity of $DiIC_{16}$, $DiIC_{12}$, and C_6-NBD-SM at normal cholesterol concentration and a nonuniform intensity at decreased cholesterol concentration (at 34°C). After decreasing the cholesterol concentration (40% of total normal cell cholesterol) at least two different environments were observed: one enriched in $DiIC_{16}$ and the other enriched in $DiIC_{12}$ and C_6-NBD-SM. Based on FRAP measurements, the diffusion of C_6-NBD-SM in the areas enriched in C_6-NBD-SM was slower after cholesterol reduction. Kenworthy et al. observed an ~2-fold decrease in diffusion for all studied proteins at ~30% normal cholesterol concentration, and no change in diffusion after an ~2-fold increase in cholesterol concentration above normal (Kenworthy et al., 2004). It is interesting to note that Kenworthy et al. (2004) observed the above effect at 37°C. The results of our current work differ from those of Pralle et al. (2000) and Shvartsman et al (2003), where an increase in diffusion coefficients was observed upon cholesterol depletion. In these studies, the effect of varying the cholesterol concentration on diffusion might have yielded different results due to differences in the exact cholesterol concentrations and temperatures (37°C in Pralle et al. versus 22°C in Shvartsman et al. and in our study) at which experiments were conducted, which is consistent with the cholesterol concentration and temperature effects observed by Smith and McConnell (Smith et al., 1980).

In conclusion it will be noted that the rate of loss of cholesterol from the cell membrane depends on the chemical activity of cholesterol. More specifically, the probability that any given cholesterol molecule leaves the membrane (specific loss rate) depends on the activity coefficient of the cholesterol molecule. Assuming, as before, that the normal state of the membrane corresponds to an equivalence composition, it will be seen that in general the loss rate will be biphasic, the proportion of fast component depending on the shape of the activity versus composition curve. From a qualitative perspective, this expectation is consistent with the data given in Fig. 1 *A*, where a biphasic loss of cholesterol is observed. This result has also been obtained in other laboratories (Kilsdonk et al., 1995; Haynes et al., 2000; Steck et al., 2002). It should be noted that a biphasic loss rate does not require the presence of distinct macroscopic ''pools'' of cholesterol, and is consistent with the presence of complexes between cholesterol and phospholipids in cell membranes. It should also be noted that the presence of proteins in cell membranes in no way invalidates these arguments, which are quite general.

SUPPLEMENTARY MATERIAL

An online supplement to this article can be found by visiting BJ Online at http://www.biophysj.org.

The authors thank Arun Radhakrishnan for helpful discussions.

This work was supported in part by grant 5R01AI13587-26 from the National Institutes of Health (to H.M.M.) and in part by grant MCB-0212503 from the National Science Foundation (to W.E.M.).

REFERENCES

Almeida, P. F., W. L. Vaz, and T. E. Thompson. 1992. Lateral diffusion in the liquid phases of dimyristoylphosphatidylcholine/cholesterol lipid bilayers: a free volume analysis. *Biochemistry.* 31:6739–6747.

Alsat, E., P. Wyplosz, A. Malassine, J. Guibourdenche, D. Porquet, C. Nessmann, and D. Evain-Brion. 1996. Hypoxia impairs cell fusion and differentiation process in human cytotrophoblast, in vitro. *J. Cell. Physiol.* 168:346–353.

Anderson, H. A., E. M. Hiltbold, and P. A. Roche. 2000. Concentration of MHC class II molecules in lipid rafts facilitates antigen presentation. *Nat. Immunol.* 1:156–162.

Anderson, R. G. W. 1998. The caveolae membrane system. *Annu. Rev. Biochem.* 67:199–225.

Anderson, R. G. W., and K. Jacobson. 2002. A role for lipid shells in targeting proteins to caveolae, rafts and other lipid domains. *Science.* 296:1821–1825.

Arni, S., S. A. Keilbaugh, A. G. Ostermeyer, and D. Brown. 1998. Association of GAP-43 with detergent -resistant membranes requires two palmitoylated cysteine residues. *J. Biol. Chem.* 273:28478–28485.

Benting, J., A. Rietveld, I. Ansorge, and K. Simons. 1999. Acyl and alkyl chain length of GPI-anchors is critical for raft association in vitro. *FEBS Lett.* 462:47–50.

Brown, D., and J. K. Rose. 1992. Sorting of GPI-anchored proteins to glycolipid-enriched membrane subdomains during transport to the apical cell surface. *Cell.* 68:533–544.

Brown, D. A., and E. London. 1998. Functions of lipid rafts in biological membranes. *Annu. Rev. Cell Dev. Biol.* 14:111–136.

Brown, D. A., and E. London. 2000. Structure and function of sphingolipid- and cholesterol-rich membrane rafts. *J. Biol. Chem.* 275:17221–17224.

Daniliuc, S., H. Bitterman, M. A. Rahat, A. Kinarty, D. Rosenzweig, and L. Nitza. 2003. Hypoxia inactivates inducible nitric oxide synthase in mouse macrophages by disrupting its interaction with alpha-actinin 4. *J. Immunol.* 171:3225–3232.

Dietrich, C., B. Yang, T. Fujiwara, A. Kusumi, and K. Jacobson. 2002. Relationship of lipid rafts to transient confinement zones detected by single particle tracking. *Biophys. J.* 82:274–284.

Feder, T. J., I. Brust-Mascher, J. P. Slattery, B. Baird, and W. W. Webb. 1996. Constrained diffusion of immobile fraction on cell surfaces: a new interpretation. *Biophys. J.* 70:2767–2773.

Feingold, L. 1993. Cholesterol in Membrane Models. CRC Press, Ann Arbor, MI.

Field, K., D. Holowka, and B. Baird. 1997. Compartmentalized activation of the high affinity immunoglobulin E receptor within membrane domains. *J. Biol. Chem.* 272:4276–4280.

Fujiwara, T., K. Ritchie, H. Murakoshi, K. Jacobson, and A. Kusumi. 2002. Phospholipids undergo hop diffusion in compartmentalized cell membrane. *J. Cell Biol.* 157:1071–1081.

Hao, M., S. Mukherjee, and F. R. Maxfield. 2001. Cholesterol depletion induces large scale domain segregation in living cell membranes. *Proc. Natl. Acad. Sci. USA.* 98:13072–13077.

Harder, T., and M. Kuhn. 2000. Selective accumulation of raft-associated membrane protein LAT in T cell receptor signaling assemblies. *J. Cell Biol.* 151:199–207.

Harder, T., P. Scheiffele, P. Verkade, and K. Simons. 1998. Lipid domain structure of the plasma membrane revealed by patching of membrane components. *J. Cell Biol.* 141:929–942.

Haynes, M. P., M. C. Phillips, and G. H. Rothblad. 2000. Efflux of cholesterol from different cellular pools. *Biochemistry.* 39:4508–4517.

Hiltbold, E. M., N. J. Poloso, and P. A. Roche. 2003. MHC class II-peptide complexes and APC lipid rafts accumulate at the immunological synapse. *J. Immunol.* 170:1329–1338.

Huby, R. D. J., R. J. Dearman, and I. Kimber. 1999. Intracellular phosphotyrosine induction by major histocompatibility complex class II requires co-aggregation with membrane rafts. *J. Biol. Chem.* 274:22591–22596.

Huby, R. D. J., A. Weiss, and S. C. Ley. 1998. Nocodazole inhibits signal transduction by the T cell antigen receptor. *J. Biol. Chem.* 273:12024–12031.

Hughes, B. D., B. A. Pailthorpe, and L. R. White. 1981. The translational and rotational drag on a cylinder moving in a membrane. *J. Fluid Mech.* 110:349–372.

Kenworthy, A. K., B. J. Nichols, C. L. Remmert, G. M. Hendrix, M. Kumar, J. Zimmerberg, and J. Lippincott-Schwartz. 2004. Dynamics of putative raft-associated proteins at the cell surface. *J. Cell Biol.* 165:735–746.

Kenworthy, A. K., N. Petranova, and M. Edidin. 2000. High-resolution FRET microscopy of cholera-toxin B-subunit and GPI- anchored proteins in cell plasma membranes. *Mol. Biol. Cell.* 11:1645–1655.

Kilsdonk, E. P. C., P. G. Yancey, G. W. Stoudt, E. Wen Bangerter, W. J. Johnson, M. C. Phillips, and G. H. Rothblad. 1995. Cellular cholesterol efflux mediated by cyclodextrins. *J. Biol. Chem.* 270:17250–17256.

Kwik, J., S. Boyle, D. Fooksman, L. Margolis, M. P. Sheetz, and M. Edidin. 2003. Membrane cholesterol, lateral mobility, and the phosphatidylinositol 4,5-bisphosphate-dependent organization of cell actin. *Proc. Natl. Acad. Sci. USA.* 100:13964–13969.

Lange, Y. 1991. Disposition of intracellular cholesterol in human fibroblasts. *J. Lipid Res.* 32:329–339.

Lange, Y., J. Ye, and T. L. Steck. 2004. How cholesterol homeostasis is regulated by plasma membrane cholesterol in excess of phospholipids. *Proc. Natl. Acad. Sci. USA.* In press.

McConnell, H. M., and A. Radhakrishnan. 2003. Condensed complexes of cholesterol and phospholipids. *Biochim. Biophys. Acta.* 1610:159–173.

McConnell, H. M., and M. Vrljic. 2003. Liquid-liquid immiscibility in membranes. *Annu. Rev. Biophys. Biomol. Struct.* 32:469–492.

Moerner, W. E., and D. P. Fromm. 2003. Methods of single-molecule fluorescence spectroscopy and microscopy. *Rev. Sci. Instrum.* 74:3597–3619.

Moffett, S., D. A. Brown, and M. E. Linder. 2000. Lipid-dependent targeting of G proteins into rafts. *J. Biol. Chem.* 275:2191–2198.

Murakoshi, H., R. Iino, T. Kobayashi, T. Fujiwara, C. Ohshima, A. Yoshimura, and A. Kusumi. 2004. Single-molecule imaging analysis of Ras activation in living cells. *Proc. Natl. Acad. Sci. USA.* 101:7317–7322.

Murase, K., T. Fujiwara, Y. Umemura, K. Suzuki, R. Iino, H. Yamashita, M. Saito, H. Murakoshi, K. Ritchie, and A. Kusumi. 2004. Ultrafine membrane compartments for molecular diffusion as revealed by single molecule techniques. *Biophys. J.* 86:4075–4093.

Neufeld, E. B., A. M. Cooney, J. Pitha, E. A. Dawidowicz, N. K. Dwyer, P. G. Pentchev, and E. J. Blanchette-Mackie. 1996. Intracellular trafficking of cholesterol monitored with a cyclodextrin. *J. Biol. Chem.* 271:21604–21613.

Nurko, S., K. Sogabe, J. A. Davis, N. F. Roeser, M. Defrain, A. Chien, D. Hinshaw, B. They, W. Meixner, M. A. Venkatachalam, and J. M. Weinberg. 1996. Contribution of actin cytoskeletal alterations to ATP depletion and calcium-induced proximal tubule cell injury. *Am. J. Physiol.* 270:F39–F52.

Pralle, A., P. Keller, E. L. Florin, K. Simons, and J. K. H. Horber. 2000. Sphingolipid-cholesterol rafts diffuse as small entities in the plasma membrane of mammalian cells. *J. Cell Biol.* 148:997–1007.

Qian, H., M. P. Sheetz, and E. L. Elson. 1991. Single particle tracking. Analysis of diffusion and flow in two-dimensional systems. *Biophys. J.* 60:910–921.

Rabinowitz, J. D., J. F. Vacchino, C. Beeson, and H. M. McConnell. 1998a. Potentiometric measurement of intracellular redox activity. *J. Am. Chem. Soc.* 120:2464–2473.

Rabinowitz, J. D., M. Vrljic, P. M. Kasson, J. J. Boniface, M. M. Davis, and H. M. McConnell. 1998b. Formation of a highly peptide-receptive state of class II MHC. *Immunity.* 9:699–709.

Radhakrishnan, A., and H. M. McConnell. 1999. Condensed complexes of cholesterol and phospholipids. *Biophys. J.* 77:1507–1517.

Radhakrishnan, A., and H. M. McConnell. 2000a. Chemical activity of cholesterol in membranes. *Biochemistry.* 39:8119–8124.

Radhakrishnan, A., and H. M. McConnell. 2000b. Electric field effect on cholesterol-phospholipid complexes. *Proc. Natl. Acad. Sci. USA.* 97:1073–1078.

Redman, C. A., J. E. Thomas-Oates, S. Ogata, Y. Ikehara, and M. A. J. Ferguson. 1994. Structure of the glycosylphosphatidylinositol membrane anchor of human placental alkaline phosphatase. *Biochem. J.* 302:861–865.

Rotsch, C., and M. Radmacher. 2000. Drug-induced changes of cytoskeletal structure and mechanics in fibroblasts: an atomic microscopy study. *Biophys. J.* 78:520–535.

Saffman, P. G., and M. Delbruck. 1975. Brownian motion in biological membranes. *Proc. Natl. Acad. Sci. USA.* 72:3111–3113.

Saxton, M. J. 1990. Lateral diffusion in a mixture of mobile and immobile particles A Monte Carlo study. *Biophys. J.* 58:1303–1306.

Saxton, M. J. 1992. Lateral diffusion and aggregation: a Monte Carlo study. *Biophys. J.* 61:119–128.

Saxton, M. J. 1993. Lateral diffusion in an archipelago. single-particle diffusion. *Biophys. J.* 64:1766–1780.

Saxton, M. 1994. Anomalous diffusion due to obstacles: a Monte Carlo study. *Biophys. J.* 66:394–401.

Saxton, M. J. 1995. Single-particle tracking: effects of corrals. *Biophys. J.* 69:389–398.

Saxton, M. J. 1997. Single-particle tracking: the distribution of diffusion coefficients. *Biophys. J.* 72:1744–1753.

Scheiffele, P., M. G. Roth, and K. Simons. 1997. Interaction of influenza virus haemagglutinin with sphingolipid-cholesterol membrane domains via its transmembrane domain. *EMBO J.* 16:5501–5508.

Schütz, G. J., G. Kada, V. P. Pastushenko, and H. Schindler. 2000. Properties of lipid microdomains in muscle cell membrane visualized by single molecule microscopy. *EMBO J.* 19:892–901.

Sheets, E. D., D. Holowka, and B. Baird. 1999. Critical role for cholesterol in Lyn-mediated tyrosine phosphorylation of FcεRI and their association with detergent-resistant membranes. *J. Cell Biol.* 145:877–887.

Shvartsman, D. E., M. Kotler, R. D. Tall, M. G. Roth, and Y. I. Henis. 2003. Differently anchored influenza hemagglutinin mutants display distinct interaction dynamics with mutual rafts. *J. Cell Biol.* 163:879–888.

Simons, K., and D. Toomre. 2000. Lipid rafts and signal transduction. *Nat. Rev. Mol. Cell Biol.* 1:31–39.

Smith, L. M., J. L. Rubenstein, J. W. Parce, and H. M. McConnell. 1980. Lateral diffusion of M-13 coat protein in mixtures of phosphatidylcholine and cholesterol. *Biochemistry.* 19:5907–5911.

Smith, P. R., I. E. G. Morrison, K. M. Wilson, N. Fernandez, and R. J. Cherry. 1999. Anomalous diffusion of major histocompatibility complex class I molecules on HeLa cells determined by single particle tracking. *Biophys. J.* 76:3331–3344.

Sooksawate, T., and M. A. Simmonds. 2001. Effects of membrane cholesterol on the sensitivity of the GABA(A) receptor to GABA in acutely dissociated rat hippocampal neurones. *Neuropharmacology.* 40:178–184.

Steck, T. L., J. Ye, and Y. Lange. 2002. Probing red cell membrane cholesterol movement with cyclodextrin. *Biophys. J.* 83:2118–2125.

Su, Y., S. Edwards-Bennett, M. R. Bubb, and E. R. Block. 2003. Regulation of endothelial nitric oxide synthase by the actin cytoskeleton. *Am. J. Physiol. Cell Physiol.* 284:C1542–C1549.

Subczynski, W. K., and A. Kusumi. 2003. Dynamics of raft molecules in the cell and artificial membranes: approaches by pulse EPR spin labeling and single molecule optical microscopy. *Biochim. Biophys. Acta.* 1610:231–243.

Vacchino, J. F., and H. M. McConnell. 2001. Peptide binding to active class II MHC molecules on the cell surface. *J. Immunol.* 166:6680–6685.

Vidalain, P. O., O. Azocar, C. Servet-Delprat, C. Rabourdin-Combe, D. Gerlier, and S. Manie. 2000. CD40 signaling in human dendritic cells is initiated within membrane rafts. *EMBO J.* 19:3304–3313.

Vrljic, M., S. Y. Nishimura, S. Brasselet, W. E. Moerner, and H. M. McConnell. 2002. Translational diffusion of individual class II MHC membrane proteins in cells. *Biophys. J.* 83:2681–2692.

Vrljic, M., S. Y. Nishimura, W. E. Moerner, and H. M. McConnell. 2003. The effect of varying cholesterol concentrations on the translational diffusion of individual class II MHC membrane proteins in cells. *Biophys. J.* 84:325A.

Wakatsuki, T., B. Schwab, N. C. Thompson, and E. L. Elson. 2000. Effects of cytochalasin D and latrunculin B on mechanical properties of cells. *J. Cell Sci.* 114:1025–1036.

Warnock, D. E., C. Roberts, M. S. Lutz, B. W.A., W. W. J. Young, and J. U. Baenziger. 1993. Determination of plasma membrane lipid mass and composition in cultured Chinese hamster ovary cells using high gradient magnetic affinity chromatography. *J. Biol. Chem.* 268:10145–10153.

Wettstein, D. A., J. J. Boniface, P. A. Reay, H. Schild, and M. M. Davis. 1991. Expression of a class II major histocompatibility complex (MHC) heterodimer in a lipid-linked form with enhanced peptide/soluble MHC complex formation at low pH. *J. Exp. Med.* 174:219–228.

Xavier, R., T. Brennan, Q. Li, C. McCormack, and B. Seed. 1998. Membrane compartmentation is required for efficient T cell activation. *Immunity.* 8:723–732.

Yguerabide, J., J. A. Schmidt, and E. E. Yguerabide. 1982. Lateral mobility in membranes as detected by fluorescence recovery after photobleaching. *Biophys. J.* 39:69–75.